IEEE Photonics Journal
An IEEE Photonics Society Publication

Open Access

Color-Shift Keying for Optical Camera Communication Using a Rolling Shutter Mode

Volume 11, Number 2, April 2019

Hao-Wei Chen
Shang-Sheng Wen
Xing-Lin Wang
Ming-Zhu Liang
Mu-Yun Li
Qing-Chang Li
Yun Liu

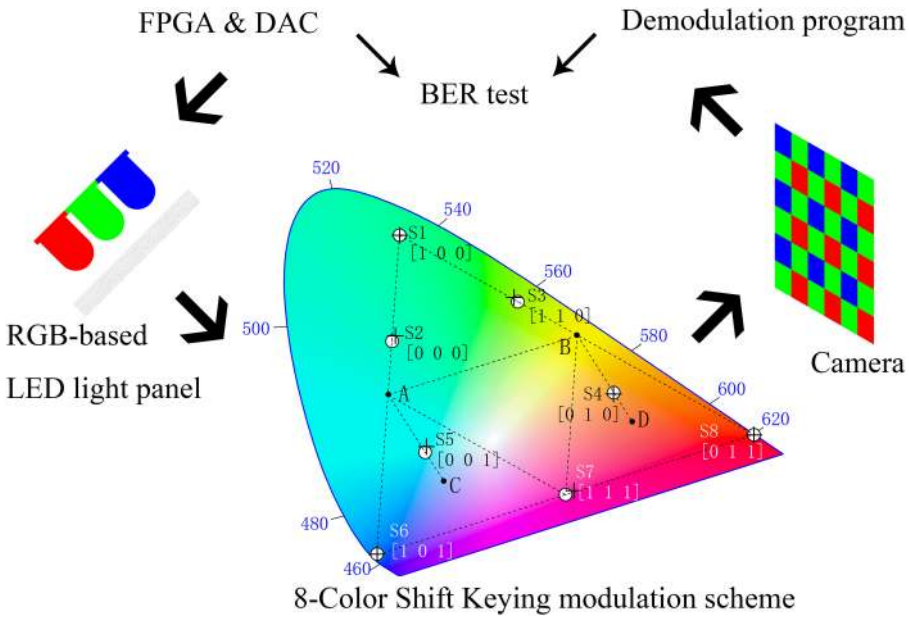

8-Color Shift Keying modulation scheme

DOI: 10.1109/JPHOT.2019.2898909
1943-0655 © 2019 IEEE

IEEE photonics SOCIETY

IEEE

Color-Shift Keying for Optical Camera Communication Using a Rolling Shutter Mode

Hao-Wei Chen,[1,2] Shang-Sheng Wen,[1,2] Xing-Lin Wang,[1] Ming-Zhu Liang,[1] Mu-Yun Li,[1,2] Qing-Chang Li,[1,2] and Yun Liu[1,2]

[1]School of Materials Science and Engineering, South China University of Technology, Guangzhou 510640, China
[2]State Key Laboratory of Luminescence Materials and Devices, South China University of Technology, Guangzhou 510640, China

DOI:10.1109/JPHOT.2019.2898909

Manuscript received December 21, 2018; accepted February 8, 2019. Date of publication February 12, 2019; date of current version March 4, 2019. This work was supported in part by the Guangdong Province Science and Technology Project under Grants 2015B010127004, 2015B010134001, 201604016010, 201604040004, 201704030140, and 2017B010114001; in part by the Zhong Shan Science and Technology Project under Grants 2016A1009 and 2017C1011; and in part by the Yang-Fan Project under Grant 2015YT02C093. Corresponding author: Shang-Sheng Wen (e-mail: shshwen@scut.edu.cn).

Abstract: An optical camera communication (OCC) is a special type of a visible light communication that uses a complementary metal-oxide semiconductor as a receiver. However, it is difficult to apply a high-order modulation scheme to such communications because of strong intersymbol interference. In this paper, we propose and demonstrate an OCC system using an 8-color color-shift keying scheme. We used an RGB-based LED light panel as a transmitter and analyzed the properties of the rolling shutter. We discuss the demodulation process and perform bit error rate (BER) tests at different ambient illuminances and sampling positions. A net data rate of 8.64 kbps and a pixel efficiency of 3.75 pixels per bit were achieved while keeping the BER below 3.8E-3, which meets the FEC's 7% forward error correction requirement. In addition, the system shows good robustness for indoor applications.

Index Terms: Optical camera communication (OCC), color-shift keying (CSK), light emitting diode (LED), light panel, rolling shutter.

1. Introduction

Complementary-Metal-Oxide-Semiconductor (CMOS)-based optical cameras are widely used; thus, it would be interesting to utilize these cameras for small-scale data transmissions [1], [2]. Wireless communications using optical cameras as receivers, called optical camera communication (OCC), has attracted considerable attention. OCC is a special type of visible light communication (VLC) that uses rapidly changing visible light produced by light emitting diodes (LEDs) to carry information and an optical camera to receive the light signals [1]–[4]. By using light panels as transmitters (Tx) [5], [6], received images will have higher quality than Tx using LED point sources, which makes the decoding process easier. An on–off keying (OOK) modulation scheme and phosphor-based white-light LED are widely utilized in OCC systems [7]–[10]. This modulation scheme is relatively easy to demodulate with a good bit error rate (BER) because it has only two voltage levels. Chow

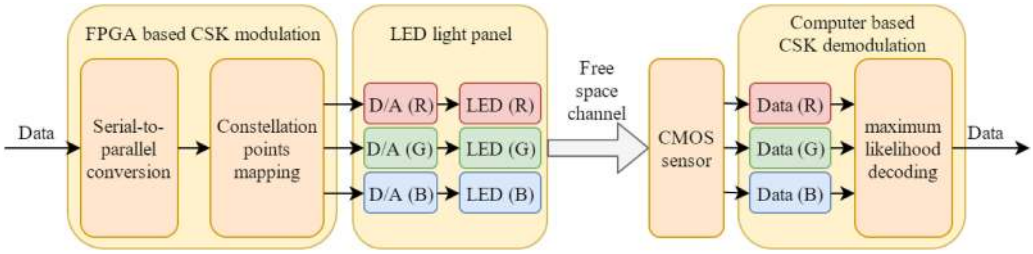

Fig. 1. Experimental configuration.

et al. proposed an OCC system with a data rate of 5.76 kb/s at 60 frames per second (fps) with a resolution of 1,920 × 1,080 pixels that achieved 11.25 pixels per bit [9]. Wang *et al.* also achieved a high data rate of 10.32 Kbps at 60 fps with a resolution of 1,920 × 1,080 pixels using one color that reached 6.28 pixels per bit [4].

Color-shift keying (CSK) is a VLC modulation scheme recommended by the IEEE 802.15.7 task group [11] that has been widely researched for several years [12]–[15]. The 8-CSK modulation scheme can greatly improve communication efficiency. Unlike OOK, there are more than two symbols; thus, the data rate can potentially be increased [16]. Three logical bits are represented by one symbol in our work. The data rate can be improved by using a high-order modulation scheme if the symbol duration time, or baud rate, remains the same. However, to achieve a low symbol error rate, a longer symbol duration time is required. If the extended symbol duration time is less than 3 times the original duration time, it will be profitable. The electro-optic conversion characteristics of LEDs of different colors are different, and LEDs must output a variety of brightness magnitudes to synthesize certain colors. Pengfei Luo *et al.*, demonstrated an OCC system using an 8-CKS modulation scheme and a 50 fps camera, achieving a data rate of 150 bits/s over a range of up to 60 m [14], [15]. The symbol rate was equal to the frame rate in this case. Tadahiro Wada introduced a new CSK-based OCC system [17]. A liquid crystal display (LCD) was utilized as a Tx, which displayed a 16 × 32 color matrix. Four colors (black, blue, red and purple) were used in the experiment, attaining a 1016-bit/frame result. The image sensor is operated in picture mode in this experiment.

In this paper, we propose and demonstrate an OCC system for indoor applications that uses an LED light panel as a Tx and a CMOS image sensor in rolling shutter mode as a receiver (Rx). By utilizing an 8-CSK modulation scheme and a beacon jointed packet reconstruction scheme [4], the proposed OCC system achieved a high pixel efficiency. The frame rate was 30 fps, and the resolution was 1,920 × 1,080 pixels (limited by hardware) with a pixel efficiency of 3.75 pixels per bit. The LED light panel provided better signal quality than a traditional LED point source by reducing the blooming effect of the CMOS sensor, which reduces the BER and simplifies the demodulation process. The lowest BER can reach 1.68E-3, satisfying the 7% forward error correction (FEC) limit, which is 3.8E-3.

2. Experiment and Algorithm

Fig. 1 depicts the experimental configuration, and Fig. 2 shows the Tx. An RGB LED light panel driven by a field programmable gate array (FPGA) system (Cyclone IV-E EP4CE6F17C8, Intel, USA) and its peripheral circuits was utilized as a VLC Tx. The size of the light panel is 5 cm × 5 cm. The driver mainly contained one four-channel digital-to-analog converter (DAC) (TLC5620C, Texas Instruments Incorporated, USA) and three independent constant current circuits (PT4205, Texas Instruments Incorporated, USA). A CMOS-based optical camera (IMX179, Sony, Japan) with a resolution of 1,920 × 1,080 pixels and a field of view (FOV) of 65 degrees was used as a VLC Rx. The frame rate was set to 30 fps. The data were programmed in the FPGA. The recorded videos were demodulated using a computer program.

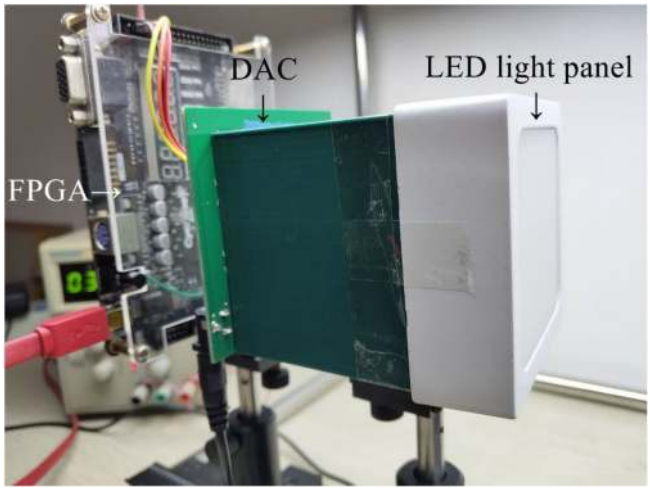

Fig. 2. The transmitter, which included an LED light panel and an FPGA-based driver.

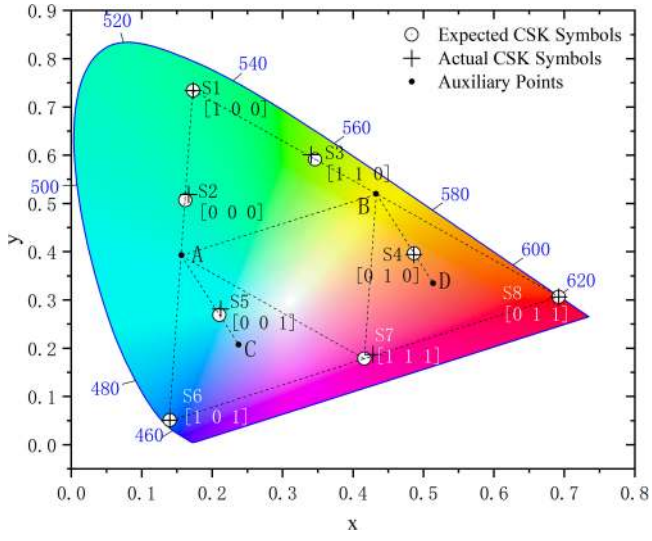

Fig. 3. Constellation diagram of 8-CSK and calibration result.

Fig. 3 shows the 8-CSK constellation definition recommended by IEEE 802.15.7 [11]. This diagram is built in CIE 1931 color space. Points S1, S6, and S8 are the CIE chromaticity coordinates of R, G and B LEDs. Points A, B, and S7 are the midpoints of the line segments, while points C and D are the centroids of triangles A-S6-S7 and B-S7-S8, respectively. Points S2, S3, S4, and S5 are the tripartite points of the line segments. Points S1, S2, S3, S4, S5, S6, S7, and S8 are the constellation points used in the experiment. Gray Code was implemented to reduce the BER, as shown in Fig. 3. The electro-optic conversion of LEDs is nonlinear. To solve this problem, we applied a calibration process to compensate for the nonlinear characters, found suitable driving current values for each symbol, and ensured that these LEDs generate the correct colors and corresponding luminance. During color calibration, we used a luminance colorimeter (SRC-200, EverFine, China) to measure the CIE chromaticity coordinates and the brightness of the light panel. The calculated and measured CIE color coordinates are shown in Fig. 3.

Usually, we assume that the transmitted data are random; thus, the probability of each symbol being transmitted is the same. Moreover, the CIE chromaticity coordinates (x_i, y_i) and luminance L_i of

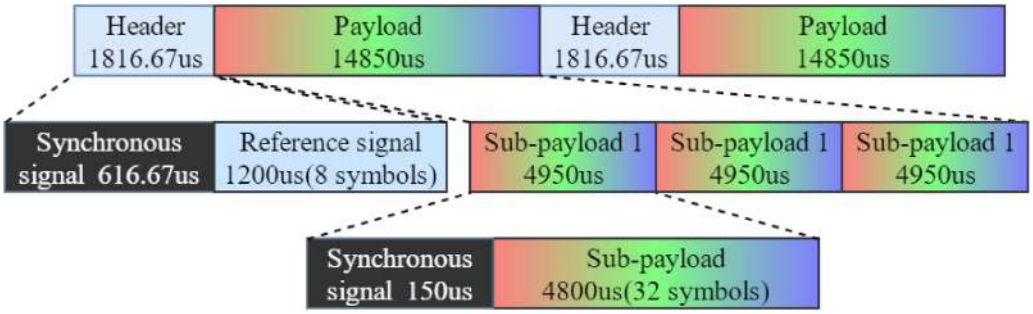

Fig. 4. Signal frame structure.

the symbols are fixed. According to the additive color-mixing theory, which is shown as Eq. (1) below, the CIE chromaticity coordinates (x_{mix}, y_{mix}) of the mixed light are constant so that the correlated color temperature of a perceived color is constant (approximately 7000K in the experiment)

$$x_{mix} = \frac{\sum_{i=1}^{8} \frac{x_i}{y_i} * \frac{L_i}{8}}{\sum_{i=1}^{8} \frac{1}{y_i} * \frac{L_i}{8}} \qquad y_{mix} = \frac{\sum_{i=1}^{8} \frac{L_i}{8}}{\sum_{i=1}^{8} \frac{1}{y_i} * \frac{L_i}{8}} \tag{1}$$

Here, x_i, y_i and L_i are the x, y chromaticity coordinates and luminance of the symbol i.

The -3-dB cut-off frequency of the monochrome LED could be higher than 10 MHz, thereby becoming the performance bottleneck of a VLC system with photodiode (PD) detector. However, the bottleneck comes from the low sampling rate and the long exposure time of the optical camera [6]. The data rate should adapt to the CMOS sampling frequency and exposure time to avoid strong intersymbol interference (ISI). The sampling frequency F_s was approximately 60 kHz, the exposure time T_e was 50 μs, and the sensitivity was set to ISO 800. Eq. (2) shows the relationship between D_0, F_s and T_e, where D_0 is the minimum undisturbed pixel distance. D_0 is expressed in pixels. Thus, theoretically, when two pixels are spaced D_0 apart, their exposures will not overlap. In this experiment, $D_0 = 4$

$$D_0 = \frac{T_e}{T_s} + 1 = T_e{}^{*} F_s + 1 \tag{2}$$

However, we found that the spacing distance should be doubled to avoid the strong ISI caused by the rolling shutter effect. Therefore, the symbol duration time was set to $9T_s$, which is approximately 150 μs. The system presented strong ISI when the symbol duration time decreased. In the 8-CSK modulation scheme, each symbol represents 3 logical bits. In other words, only 3 columns of pixels are needed to represent one logical bit, which is considerably better than the case using OOK. The Tx had a baud rate of 6.67 Bd and a data rate of 20 kb/s.

Wang *et al.* proposed a beacon jointed packet reconstruction scheme [4] that can increase the data rate by reading signals bidirectionally during the demodulation process. This approach allows longer packets to be transmitted, achieving higher data rates. The signal frame structure we used is illustrated in Fig. 4. Each frame contains two headers (also called pilot signals) and two payloads to avoid the "blind time" between two frames of the video. The header can be divided into 616.67 μs of synchronous signal and 1,200 μs of reference signal. The length of the synchronous signal was self-adaptive to ensure that the length of one frame was 1/30 s. When sending the synchronous signal, all the LEDs shut down, causing a black strip in the image. Then, 8 constellation points were transmitted in sequence as a reference for decoding. The payload can be decomposed into 3 sub-payloads. Each sub-payload contains 150 μs of synchronous signals and 4,800 μs of data (32 symbols). In other words, one frame contained 288 logical bits.

Although the CSK modulation scheme was originally designed for CIE 1931 color space, the CMOS sensor generates data in RGB color space. Thus, the demodulation was processed directly in RGB color space, which helped to reduce the algorithm's complexity. During the demodulation

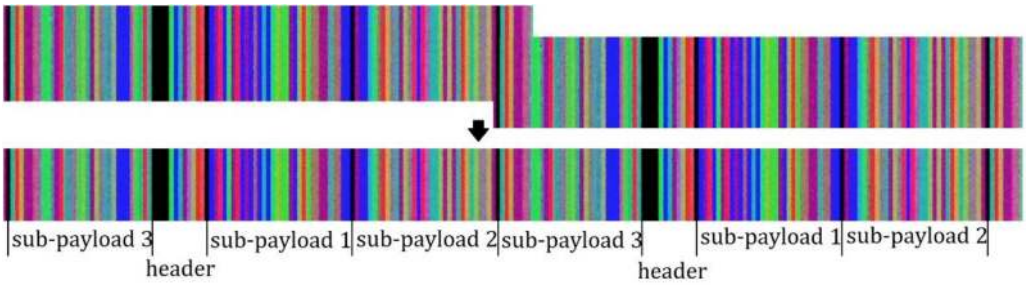

Fig. 5. A typical frame of the received signal and the beacon jointed packet reconstruction scheme.

process, we first recognized the synchronous signal in the header, which lasted 616.67 μs and was unique in the frame, allowing it to be utilized as an identifier. Then, the sub-payload can be extracted with the help of the synchronous signal lasted 150 μs. Each sub-payload included one synchronous signal that lasted for the duration of one symbol (150 us), helping clock recovery. Fig. 5 shows a typical frame and the reconstruction scheme. The background compensation blooming-mitigation algorithm [10] was applied to lessen the impact of blooming effect. The beacon jointed packet reconstruction scheme [4] was used for signal reconstruction. Symbols in the header, were used as references for the maximum likelihood (ML) demodulation algorithm because they occurred in a specified order. The sampling positions were set near the middle of the strip. The sampling positions noticeably affect the demodulation result, as described in Section 3. The quality of the pilot signal largely determines the performance of the system.

3. Result and Discussions

Here, we define a new data-rate evaluation method called pixel efficiency for OCC based on the rolling shutter effect that avoids hardware influences and evaluates the capabilities of a modulation scheme more reasonably. The number of pixels in each row is divided by the amount of net data in each frame. Thus, the dimension of pixel efficiency is pixels-per-bit. To achieve a higher data rate, we want to represent one logical bit with as few pixels as possible. Thus, pixels-per-bit is an effective unit for evaluating system quality. For example, the resolution we used was 1,920 $\times$ 1,080 pixels, where the number of pixels in each row was 1,080. In addition, 288 logical bits were recorded in one frame. Thus, the system had a pixel efficiency of 3.75 pixels per bit. The data rate was 8.64 kbps, slightly less than in [4] because the CMOS we used supports a maximum frame rate of only 30 fps, instead of 60 fps in [4]. However, the CKS modulation scheme dramatically improved the pixel efficiency: 3.75 pixels per bit was achieved in the experiment, which is much better than in [4] (6.28 pixels per bit).

The BER performance was evaluated and compared under different ambient light conditions and using different sampling positions. Both the received data and the transmitted data were compared during the test. The transmitted distance was fixed at 4 cm to ensure that all the pixels could receive the light from the panel directly. Ambient illuminance was measured by an illuminometer (1332A, TES, China). The spectral power distribution of ambient light, which was detected by a spectral illuminometer (spic2000, EVERFINE, China) when the illuminance was 1000 lx, is shown below in Fig. 6. The light provided a phosphor-based white-light LED luminaire, which had a correlated color temperature of approximately 6350K. The LED luminaire was driven by a high-precision constant current source to minimize its channel noise. Fig. 6 also provides the amplitude fluctuation ratios of the ambient light received by the PD (the orange line) and the CMOS image sensors (the red, green and blue lines correspond to the red, green and blue channels of the sensor). The fluctuation ratio of the orange line is much smaller than those of the others, suggesting that noise from the CMOS sensor is much greater than that from the ambient light when the film speed is ISO 800, which we used in the experiment. Moreover, the photo-diode-based signal receiving circuit and

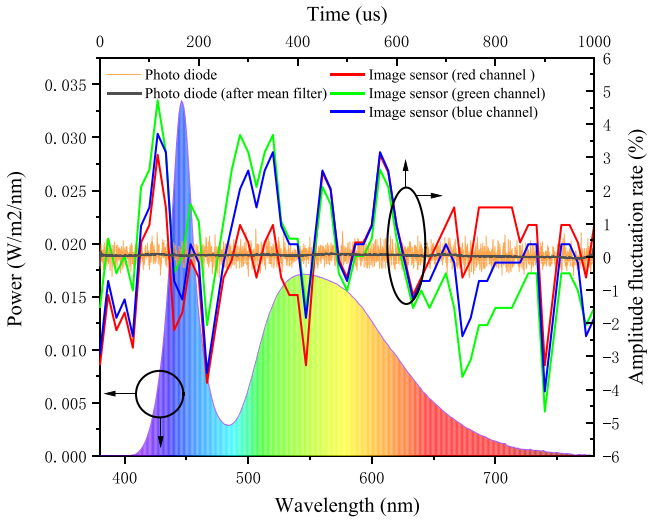

Fig. 6. Spectral power distribution of the ambient light and amplitude fluctuation ratio of the received signal.

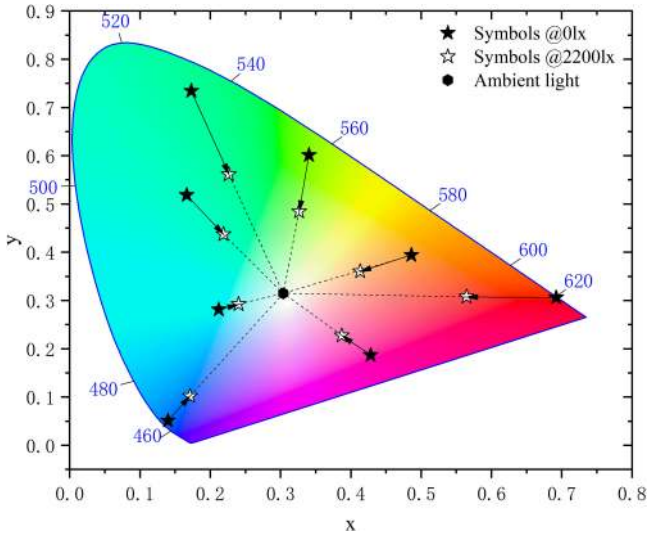

Fig. 7. Compression of the constellation diagram at 0 lx and 2,200 lx.

oscilloscope have their own noises, which are unrelated to the ambient light, leading to a fluctuation of the waveform in orange. Thus, the fluctuation of ambient light illumination was small. Although the effect on the frequency characteristics of ambient light to CSK is different for red, green, and blue channels, we assume that this effect is ignorable since the channel noise is small at different frequencies and ambient illuminances (relative to the noise from the CMOS sensor). Additionally, the exposure time of the sensor was quite long (up to 50 us), and it is like mean filter (filtering out high-frequency noise). The black line in Fig. 6 is the PD signal filtered by a 50-us mean filter.

Fig. 7 shows the constellation diagram when the ambient illuminance is 0 lx and 2,400 lx. The circles represent the reference, and the points represent the received symbols. The ML algorithm can effectively distinguish most of the signal points. When the ambient illuminance increases, light from the environment (usually white light) mixes with the light from the light panel. According to the additive color-mixing theory, shown in Eq. (3), the CIE chromaticity coordinates (x'_i, y'_i) of the mixed

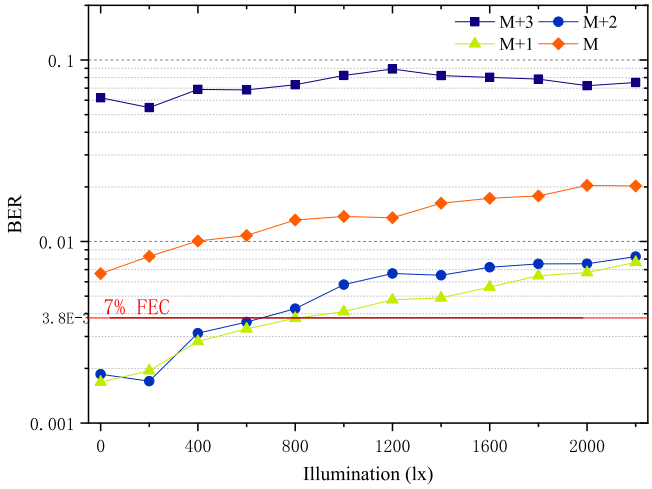

Fig. 8. Measured BER performances at diverse ambient illuminances.

colors will be located between the two original CIE chromaticity coordinates (x_i, y_i) and (x_a, y_a), causing compression of the constellation diagram (i.e., the distances between constellation points decrease). The variance of each constellation point, due to the sensor's noise, is unchanged. As regard to RGB color space, all three components increase at the same time, and the minimum Euclidean Distance decreases, causing the system BER to increase. As shown in Fig. 7, all the constellation points moved towards the center of the diagram. To reduce this effect, the LED light panel should have high brightness (in our case, the brightness was 930 cd/m^2). A brighter light panel would reduce the proportion of ambient light received by the camera

$$x_i' = \frac{\frac{x_i}{y_i}L_i + \frac{x_a}{y_a}L_a}{\frac{L_i}{y_i} + \frac{L_a}{y_a}} \qquad y_i' = \frac{L_i + L_a}{\frac{L_i}{y_i} + \frac{L_a}{y_a}} \tag{3}$$

Here, x_i, y_i and L_i are the x, y chromaticity coordinates and luminance of the symbol i, and x_a, y_a and L_a are the x, y chromaticity coordinates and luminance of the light panel when the luminaire is turned off.

Fig. 8 shows the result of the BER test. We evaluated four sampling positions, and the corresponding ambient illuminances were 0 lx, 200 lx, 400 lx, . . . , 2,200 lx. The "M" symbol in Fig. 8 denotes sampling positions in the middle of the stripe, while "M+1" denotes moving one pixel in the time direction from the "M" position and so on. A line for the 7% FEC limit also appears in Fig. 8. The system achieved the best BER performance when the sampling position was M+1. This value meets the 7% FEC limit at illumination levels lower than 800 lx. In radio frequency communication, the middle of the symbol duration time is usually sampled to obtain a lower BER. However, in OCC, the position of the sampling point should be postponed, allowing the signal more time to reach a steady state. The ability to reach steady state is an important reason why we did not use a shorter period. A larger symbol duration time provides a greater margin for sampling, which is important for achieving more accurate timing. The symbol duration time is very sensitive to the sampling position.

The blooming effect is an important issue that prevents the use of a higher order modulation scheme. The LED light panel played an important role in this experiment by allowing us to obtain a clear signal. With the help of the light panel, higher order modulation schemes such as 8-CKS can be realized, resulting in higher OCC system data rates. However, the strong ISI remains an unconquered problem. When the spacing distance was reduced—to even eight—the BER increased rapidly, far exceeding the 7% FEC limit.

When the ambient illuminance is lower than 800 lx, the system achieved a BER lower than 3.8E-3, satisfying the requirement of the 7% FEC limit. Thus, the system can meet the needs of

indoor applications, as indoor illumination is usually lower than 800 lx, and we have concluded that the system had good robustness for indoor applications. The CSK modulation scheme's error performance was worse than that of the OOK modulation scheme, as it has a smaller minimum constellation point distance. However, there is a trade-off between data rate and error performance.

4. Conclusion

In this article, we proposed and demonstrated an OCC system for indoor applications that uses an LED light panel as a Tx and a CMOS image sensor as an Rx. The Rx had a resolution of 1,920 $\times$ x1,080 pixels and a frame rate of 30 fps. The beacon jointed packet reconstruction scheme and the 8-CSK modulation scheme were adopted to improve the data rate. Three columns of pixels were used to represent one logical bit, achieving a pixel efficiency of 3.75 pixels per bit at a net data rate of 8.64 kbps (288 bits per frame). The proposed system showed good robustness for indoor applications. The system achieved its best BER performance of 1.68E-3 when the ambient illuminance was 0 lx and the sampling point was M+1, which meets the 7% FEC requirement.

References

[1] C. Chen *et al.*, "Efficient demodulation scheme for rolling-hutter-patterning of CMOS image sensor based visible light communications," *Opt. Exp.*, vol. 25, no. 20, pp. 24362–24367, 2017.
[2] J. H. Bae, N. T. Le, and J. T. Kim, "Smartphone image receiver architecture for optical camera communication," *Wireless Personal Commun.*, vol. 93, no. 4, pp. 1043–1066, 2017.
[3] N. T. Le, M. A. Hossain, and Y. M. Jang, "A survey of design and implementation for optical camera communication," *Signal Process., Image Commun.*, vol. 53, pp. 95–109, 2017.
[4] W. Wang *et al.*, "Beacon jointed packet reconstruction scheme for mobile-phone based visible light communications using rolling shutter," *IEEE Photon. J.*, vol. 9, no. 6, Dec. 2017, Art. no. 7907606.
[5] C. Chow *et al.*, "Secure mobile-phone based visible light communications with different noise-ratio light-panel," *IEEE Photon. J.*, vol. 10, no. 2, Apr. 2018, Art. no. 7902806.
[6] H. Chen *et al.*, "Optics camera communication for mobile payments using an LED panel light," *Appl. Opt.*, vol. 57, no. 19, pp. 5288–5294, 2018.
[7] Y. Liu *et al.*, "Comparison of thresholding schemes for visible light communication using mobile-phone image sensor," *Opt. Exp.*, vol. 24, no. 3, pp. 1973–1978, 2016.
[8] C. Chow, C. Chen, and S. Chen, "Enhancement of signal performance in LED visible light communications using mobile phone camera," *IEEE Photon. J.*, vol. 7, no. 5, Oct. 2015, Art. no. 7903607.
[9] K. Liang, C. Chow, and Y. Liu, "Mobile-phone based visible light communication using region-grow light source tracking for unstable light source," *Opt. Express.*, vol. 24, no. 15, pp. 17505–17510, 2016.
[10] W. Wang *et al.*, "Long distance non-line-of-sight (NLOS) visible light signal detection based on rolling-shutter-patterning of mobile-phone camera," *Opt. Exp.*, vol. 25, no. 9, pp. 10103–10108, 2017.
[11] *IEEE Standard for Local and Metropolitan Area Networks - Part 15.7: Short-Range Wireless Optical Communication Using Visible Light*, *IEEE Standard 802*, 2011.
[12] S. Chen and C. Chow, "Color-Shift keying and code-division multiple-access transmission for RGB-LED visible light communications using mobile phone camera," *IEEE Photon. J.*, vol. 6, no. 6, Dec. 2014, Art. no. 7904106.
[13] J. Okumura *et al.*, "Hybrid PWM/DPAM dimming control for digital color shift keying using RGB-LED array," *IEEE J. Sel. Areas Commun.*, vol. 36, no. 1, pp. 45–52, Jan. 2018.
[14] L. Pengfei *et al.*, "Experimental demonstration of RGB LED-based optical camera communications," *IEEE Photon. J.*, vol. 7, no. 5, Oct. 2015, Art. no. 7904212.
[15] P. Luo *et al.*, "Experimental demonstration of undersampled color-shift keying optical camera communications," in *Proc. Int. Conf. IEEE/CIC Commun.*, Qingdao, China, 2017, pp. 1–6.
[16] J. R. Won and Y. S. Soo, "RGB MIMO optical camera communication histogram equalization," in *Proc. Int. Conf. Signals Syst.*, 2017, pp. 303–307.
[17] T. Wada, H. Furukawa, and K. Mukumoto, "A study on parallel transmission wireless visible light communications using color shift keying," in *Proc. IEEE Asia Pacific Conf. Circuits Syst.*, 2014. pp. 324–327.